JAERI-Tech
2002-062

DESIGN OF EX-VESSEL NEUTRON MONITOR FOR ITER

July 2002

Takeo NISHITANI, Tetsuo IGUCHI*, Katsuyuki EBISAWA*, Michinori YAMAUCHI,
Chris WALKER* and Satoshi KASAI

日本原子力研究所
Japan Atomic Energy Research Institute

本レポートは、日本原子力研究所が不定期に公刊している研究報告書です。
入手の問合わせは、日本原子力研究所研究情報部研究情報課（〒319-1195　茨城県那珂郡東海村）あて、お申し越しください。なお、このほかに財団法人原子力弘済会資料センター（〒319-1195　茨城県那珂郡東海村日本原子力研究所内）で複写による実費頒布をおこなっております。

This report is issued irregularly.
Inquiries about availability of the reports should be addressed to Research Information Division, Department of Intellectual Resources, Japan Atomic Energy Research Institute, Tokai-mura, Naka-gun, Ibaraki-ken 319-1195, Japan.

編集兼発行　日本原子力研究所

JAERI-Tech 2002-062

Design of Ex-vessel Neutron Monitor for ITER

Takeo NISHITANI, Tetsuo IGUCHI*[1], Katsuyuki EBISAWA*[2], Michinori YAMAUCHI,
Chris WALKER*[3] and Satoshi KASAI*[1]

Department of Fusion Engineering Research
(Tokai Site)
Naka Fusion Research Establishment
Japan Atomic Energy Research Institute
Tokai-mura, Naka-gun, Ibaraki-ken

(Received May 31, 2002)

A neutron flux monitor has been designed by using ^{235}U fission chambers to be installed outside the vacuum vessel of ITER. We investigated moderator materials to get flat energy response the responses of ^{235}U fission chambers. Here we employed graphite and beryllium with a ratio of Be/C=0.25 as moderator, which materials are stable in ITER relevant temperature in a horizontal port. Based on the nuetronics calculations, a fission chamber with 200 mg of ^{235}U is adopted for the neutron flux monitor. Three detectors are mounted in a stainless steel housing with moderation material. Two fission chamber assemblies will be installed in a horizontal port; one is for D-D and calibration operation, and another is for D-T operation. The assembly for the D-D operation and the calibration are installed just outside the port plug in the horizontal port. The assembly for the D-T operation is installed just behind the additional shield in the port. Combining of those assemblies with both pulse counting mode and Campbelling mode in the electronics, a dynamic range of 10^7 can be obtained with 1 ms temporal resolution. Effects of gamma-rays and magnetic fields on the fission chamber are negligible in this arrangement. The neutron flux monitor can meet the required 10% accuracy for a fusion power monitor.

Keywords: Neutron Monitor, Fission Chamber, ITER, Fusion Power, Moderator, Diagnostics
Campbelling Mode, MCNP, Neutron Yield

This work is conducted as an ITER Engineering Activities as this report corresponds to ITER Design Task Agreement on "Diagnostics Design" (N 55 TD 02.03FJ).

+1 Department of Fusion Plasma Research
*1 Nagoya University
*2 Toshiba Corp.
*3 ITER International Team, Garching

ITER 用真空容器外中性子モニターの設計

日本原子力研究所那珂研究所核融合工学部
西谷　健夫・井口　哲夫*1・海老澤　克之*2, 山内　通則・Chris WALKER*3・河西　敏+1

(2002 年 5 月 31 日受理)

^{235}U フィッションチェンバーを用いた ITER 用の真空容器外中性子モニターの設計を行った。^{235}U フィッションチェンバーの感度が入射中性子のエネルギーに対し一定となるように減速材の設計を行った。ITER の水平ポート内の温度環境下で安定な、ベリリウムと炭素を減速材として、Be/C 比が 0.25 となるようにした。中性子輸送計算に基づき、^{235}U200mg のフィッションチェンバーを中性子検出器として採用した。３つのフィッションチェンバーをステンレス鋼のケース付きの減速材内に組み込み、１つのアセンブリとした。このアセンブリを２セット水平ポートに取付け、一つは D-D 運転と較正用、もう一つは D-T 運転用とした。D-D 運転と較正用のアセンブリは水平ポート内のポートプラグのすぐ外側に設置され、D-T 運転用アセンブリはポート中間の追加遮蔽体の陰に取付けられる。信号処理ではパルス計数方式とキャンベル方式を併用することによって、ITER の要求仕様である 10^7 のダイナミックレンジと 1ms の時間分解能を達成できることを示した。γ線と磁場の影響は、無視し得ることが解った。また、この中性子モニターは ITER の要求精度 10%を満足することを明らかにした。

本研究はＩＴＥＲ工学設計活動の一環として実施したもので、本報告は設計タスク協定(N 55 TD02. 03FJ)に基づくものである。
那珂研究所（東海駐在）：〒319-1195 茨城県那珂郡東海村白方白根 2-4

+1　炉心プラズマ研究部
*1　名古屋大学
*2　(株)東芝
*3　ITER ガルヒンク共同センター

Contents

目　次

1. INTRODUCTION

1.1 Functions

The Neutron Flux Monitors (WBS 5.5.B.04) provide essential information for plasma operation and for establishing performance characteristics. They measure the global neutron source strength, hence the total fusion power. The objectives of this work package are to review and update the initial conceptual design work undertaken for ITER-FDR98(1998ITER), and to develop the engineering design of the neutron flux monitor for ITER-FEAT.

In present large tokamaks such as JET[1], TFTR[2] or JT-60U[3], the neutron source strength measurement has been carried out using ^{235}U or ^{238}U fission chambers installed outside the vacuum vessel. ITER has a thick blanket, vacuum vessel and other equipment. Detection efficiencies of those detectors may be affected by surrounding equipment such as other diagnostics or heating systems. Therefore a fission chambers system to be installed inside the vacuum vessel (WBS 5.5.B.03) is proposed as a neutron source strength monitor for the real time fusion power control. However, we do not have any experience with the fission chambers system in the present tokamaks. So it is risky for us to rely on the fission chambers system for the real time fusion power monitor. The neutron flux monitor with ^{235}U or ^{238}U fission chambers installed outside the vacuum vessel is a well-established technique in not only present tokamaks but also other fusion devices. There the neutron flux monitor is still important on ITER-FEAT.

1.2 Design Requirements

Target measurement requirements for the Neutron Flux Monitor (5.5.B.04) are listed in Table 1.2-1. So the neutron detector has to have a wide dynamic range and a fast response. From the technical point of view, it should be robust in the ITER environment such as radiation, electro-magnetic noises, and mechanical vibrations, and not sensitive to gamma-rays. The detection efficiency must be stable in the ITER-FEAT operation life, and should be calibrated easily.

Table 1.2-1 Target Measurement Requirements.

Total Neutron Flux

Parameter	Parameter range	Spatial Resolution	Time Resolution	Accuracy
Total neutron flux	10^{13}-10^{16} n s^{-1}	integral	1 ms	20%
	10^{16}-5x10^{20} n s^{-1}	integral	1 ms	10%
Fusion power	100W-10kW	integral	1 ms	20%
	10kW-1GW	integral	1 ms	10%

1.3 Task Objectives

The specific objectives of this design phase are:

1) to re-evaluate the target measurement performance (neutron flux, fusion power, dynamic range, time resolution and accuracy);

2) to review the conceptual design(1998ITER), including the selection of neutron detectors at several points and sensitivity studies under the new ITER-FEAT configuration;

3) to complete the concept, optimize the detector position and surrounding materials, and evaluate the efficiencies and accuracy (note that the prospective locations are in ports #8 and #17 (Remote Handling ports);

4) to identify the critical interfaces with the ITER-FEAT and to design the implements for installation of the neutron flux monitors in the designated ports in collaboration with the JCT;
5) to develop the engineering design and identify the system components, cable route, and other principal auxiliary systems;

6) to design signal processing and data acquisition block diagrams, including prospective number of components, layout in the pit area and the diagnostic room;

7) to propose feasible solutions to the critical issues such as calibration of the fission chambers for the required dynamic range;

2. CONCEPT DESIGN DESCRIPTION

2.1 Basic Concept

In ITER-FDR, combination of several fission chambers with different sensitivities is proposed. They use the fission chamber only in pulse counting mode. The maximum counting rate should be less than 100 KHz. The useful dynamic range of one detector is only 10^2. The proposed system is an array of 12 detectors: two detectors each at 6 different sensitivities, with no detector from the same sensitivity pair at the same location.

For ITER-FEAT, we propose a combination of pulse counting mode and Campbelling (MSV) mode, which provides a wide dynamic range of 10^6 or more for one detector. The wide range measurement was demonstrated in JT-60 [3]. The linearity was calibrated by using a fission reactor as shown in Fig. 2.1-1, where the dynamic range of 10^7 was confirmed. Therefor we will use one kind (or two kinds) of detectors for one place.

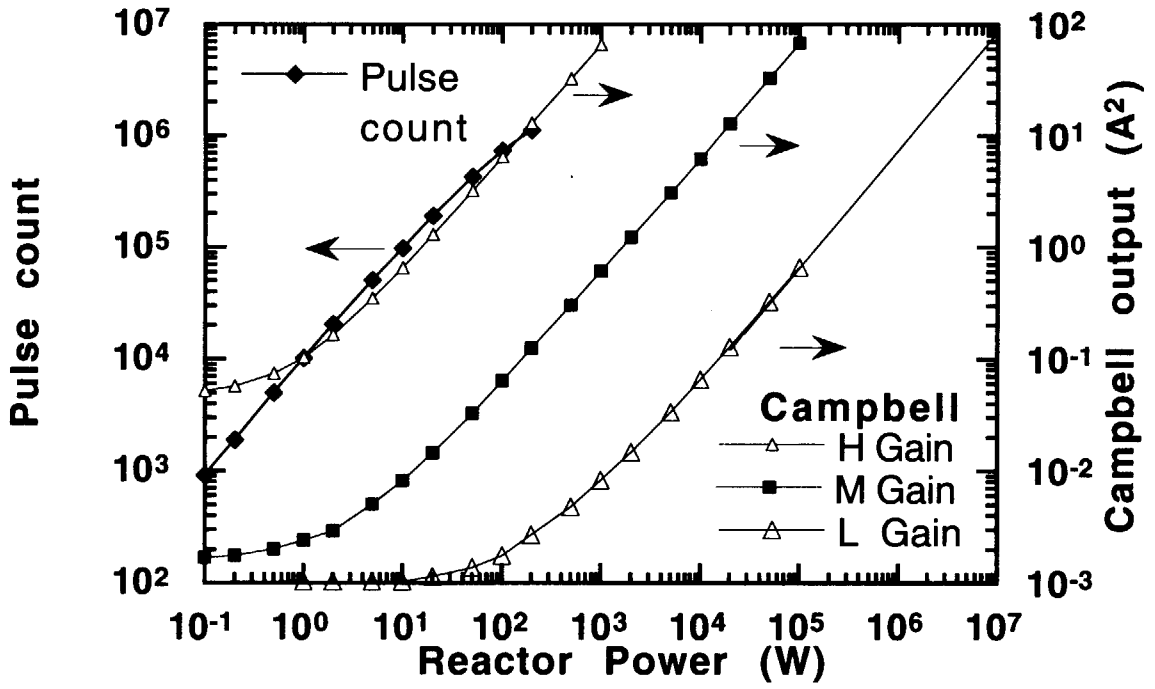

Figure 2.1-1 Linearity calibration of the JT-60U fission chamber using a fission reactor.

2.2 Fission Chamber

In ITER-FDR, three kinds of fission chambers were employed, where a variation of the sensitivity of a factor of 25×25 can be achieved between these detectors by changes in fissionable mass. The most sensitive chamber was a commercially available fission detector with up to 10 grams. For ITER-FEAT, only one type fission chamber is proposed. The variation of the sensitivity for the source neutron strength can be achieved by the variation of the location. We employed the fission chamber developed for the JT-60 neutron monitor for the ITER-FEAT neutron flux monitor.

Figure 2.2-1 shows the schematics of the typical fission chamber with wide dynamic range, which is developed for the JT-60 neutron monitor. In this detector, about 200 mg of UO_2 is coated on the cylindrical electrode and 8 atm of Ar + 5% N_2 gas is filled between the electrodes. This detector can be used under high temperature condition up to 400°C.

This fission chamber can be operated with pulse counting mode at low neutron flux, Campbelling (mean square voltage) mode[9] at medium flux and current mode at high flux. Combination of those operation modes may provide a wide dynamic range of 10^{10} with temporal resolution of 1 ms, which satisfies the ITER requirement. The most popular candidates of the fissile material in the fission chamber are ^{235}U, ^{238}U, and ^{232}Th. ^{235}U has a large fission cross-section for thermal neutrons and others occur fission event only for fast neutrons higher than ~0.8 MeV. The fission cross-section of ^{232}Th is several times lower than that of ^{238}U. So we employ ^{235}U as the fissile material for the fission chamber to get a sufficient counting rate. The fission cross-section of ^{235}U is shown in Fig.2.2-2. The performance of the fission chamber of ^{235}U with the dimensions shown in Fig.2.2-1 is listed in Table 2.2-1.

The detectors should be moderated to get a broad energy response. The design of the moderator is described in Section 2.4.

Table 2.2-1 Performance of the fission chamber with ^{235}U.

Diameter	28 mm
Total length	390 mm
Active area	140 cm^2
Fissile material	^{235}U 0.6 mg $(UO_2)/cm^2$ total 200 mg of UO_2
Enrichness of uranium	90 %
Ionizing gas	8 atm of Ar + 5% N_2
Housing material	Stainless steel 316L
Neutron sensitivity for fission reactor spectrum Pulse counting mode MSV mode DC mode	 1.2×10^{-1} cps/nv 5.7×10^{-27} A^2/Hz/nv 2×10^{-14} A/nv
Gamma sensitivity MSV mode DC mode	 7×10^{-28} A^2/Hz/R/h 2×10^{-11} A/R/h
Input voltage	100 - 300 V
Operating temperature	< 400 °C
Connector type	HN

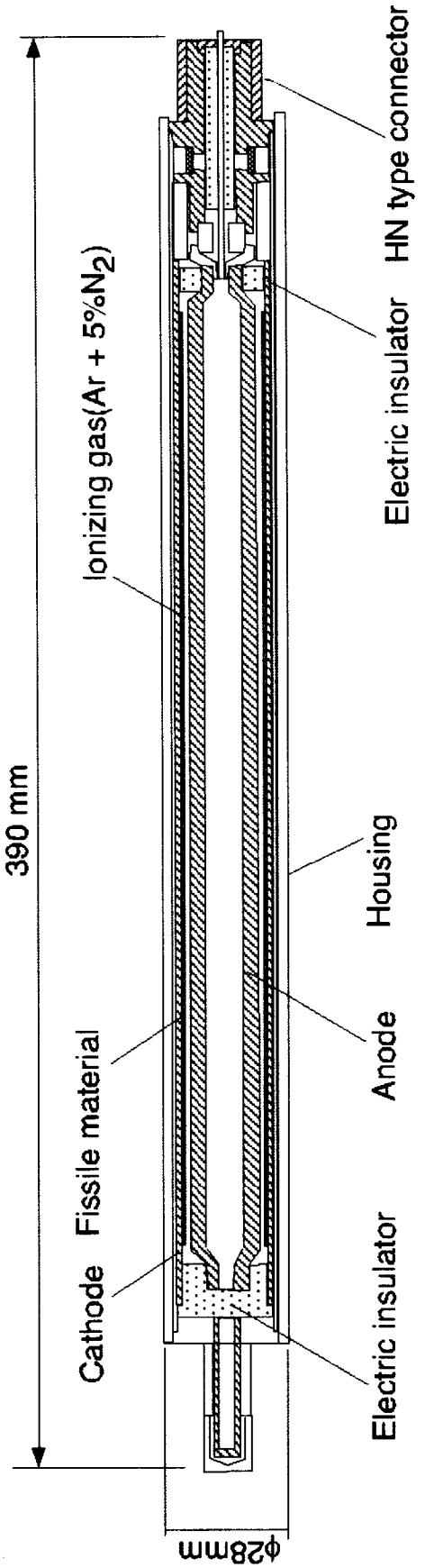

Figure 2.2-1 Schematics of the fission chamber for ITER neutron flux monitor

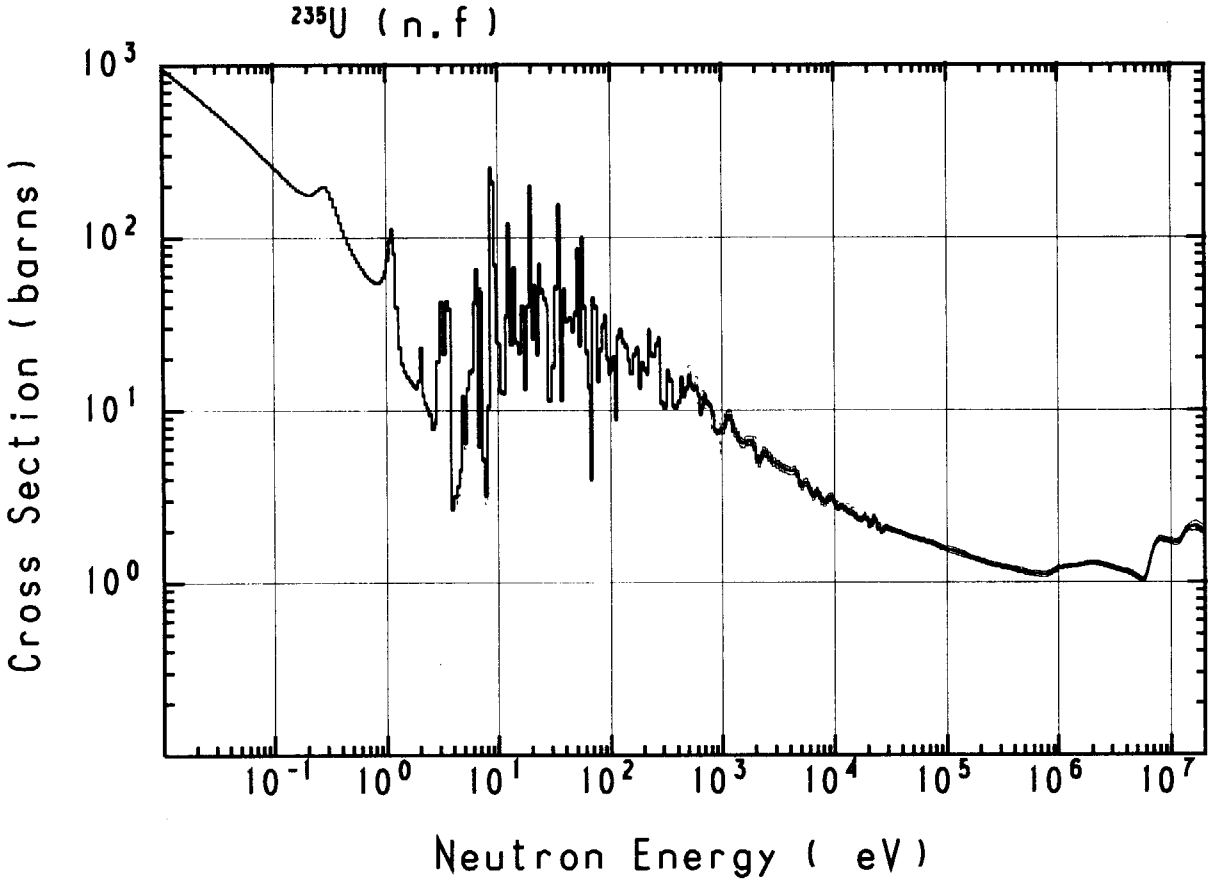

Figure 2.2-2 Fission cross-section of ^{235}U as a function of neutron energy.

2.3 Detector Location

In the ITER-FDR design, the proposed system is an array of 12 detectors: two detectors each at 6 different sensitivities, with no detector from the same sensitivity pair at the same location. Three detectors (the least sensitive for DT operation) go into a module outside the interspace vacuum on a cover plate of the secondary vacuum wall. Two detectors (the middle range of sensitivity, for ohmic and/or DD operation) go into a different module with less shielding in front of it than the least sensitive ones outside the interspace vacuum. The module of the two detectors of intermediate sensitivity is in the interspace vacuum, just outside the primary vacuum shield block. The least sensitive and middle sensitive modules can be part of the plug assembly for the limiter/RH ports.

The design of the neutron source strength monitor system requires an estimate of the local neutron flux within the bioshield of ITER. Figure 2.3-1 shows calculated neutron and gamma ray fluxes in the outboard regions during nominal operation of ITER-FEAT. The average 14 MeV neutron current at the first wall (neutron wall load) is 0.57 MW/m^2 and the resulting outboard average is 0.641 MW/m^2. Typical neutron and gamma-ray spectra at the inside surface of the vacuum vessel in the outboard are shown in Figs. 2.3-2 and 2.3-3.

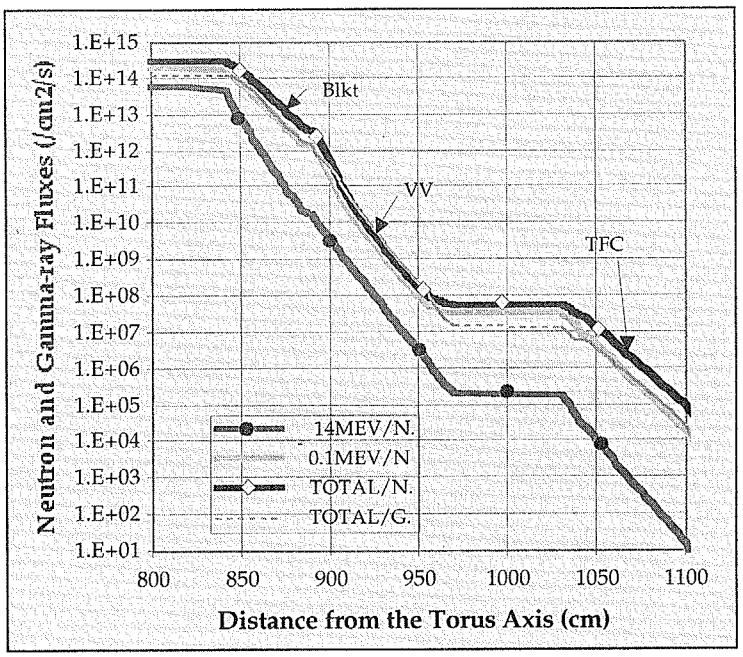

Figure 2.3-1 Neutron and Gamma-ray fluxes during operation outboard side calculated by one dimensional code.

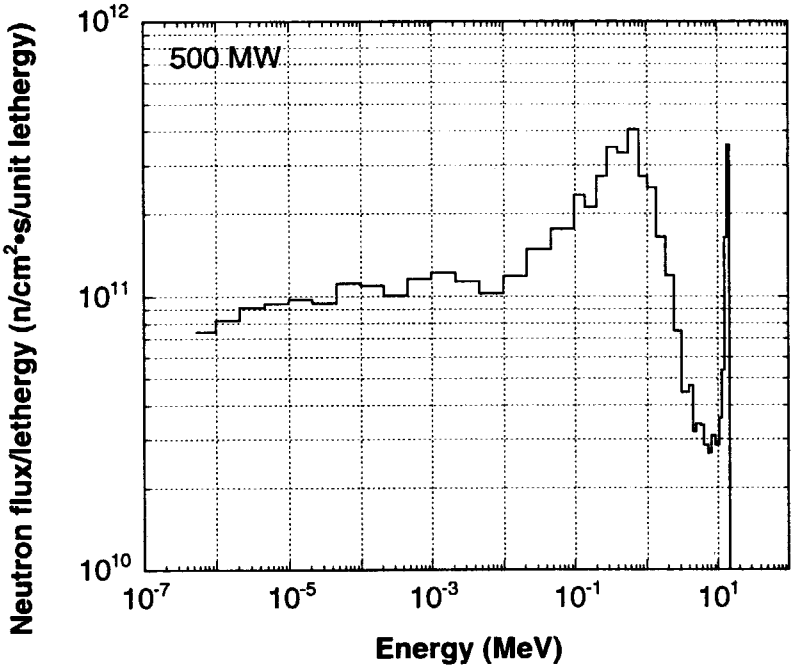

Figures 2.3-2 Typical neutron spectrum at the inside surface of the vacuum vessel in the outboard.

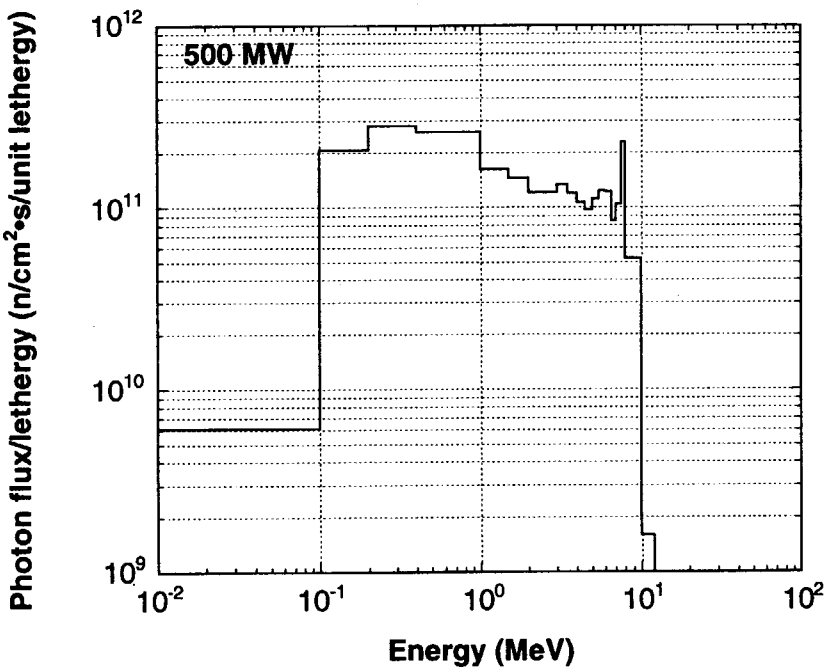

Figures 2.3-3 Typical gamma-ray spectrum at the inside surface of the vacuum vessel in the outboard.

Figure 2.3-5 shows the count rate of the fission chamber as a function of the major radius, which is estimated by the neutron flux distribution shown in Fig. 2.3-1. Enhancement of the sensitivity by a moderator was not taken into account. The count rate was calculated by $N\sigma\phi$, where N is the number of ^{235}U atoms, σ is the fission cross section and ϕ is the neutron flux. The count rate in the horizontal port was estimated by a $1/r^2$ relation, where r is the distance from the plasma axis, so called minor radius.

The detectors for the D-D operation and the calibration have to be installed as close to the plasma as possible. Taking account of the integration of other diagnostics, we decided to install the detectors for the D-D operation and the calibration in the horizontal port just outside the vacuum vessel at R~9.5m. The maximum count rate of the Campbelling mode is about 10^9 cps. So the maximum neutron flux should be ~10^{10} n/cm^2•s at the detector location at 1 GW fusion power, because the sensitivity is ~0.1 cps/nv. We decided to install the detectors for the D-T operation in the horizontal port at R~11m.

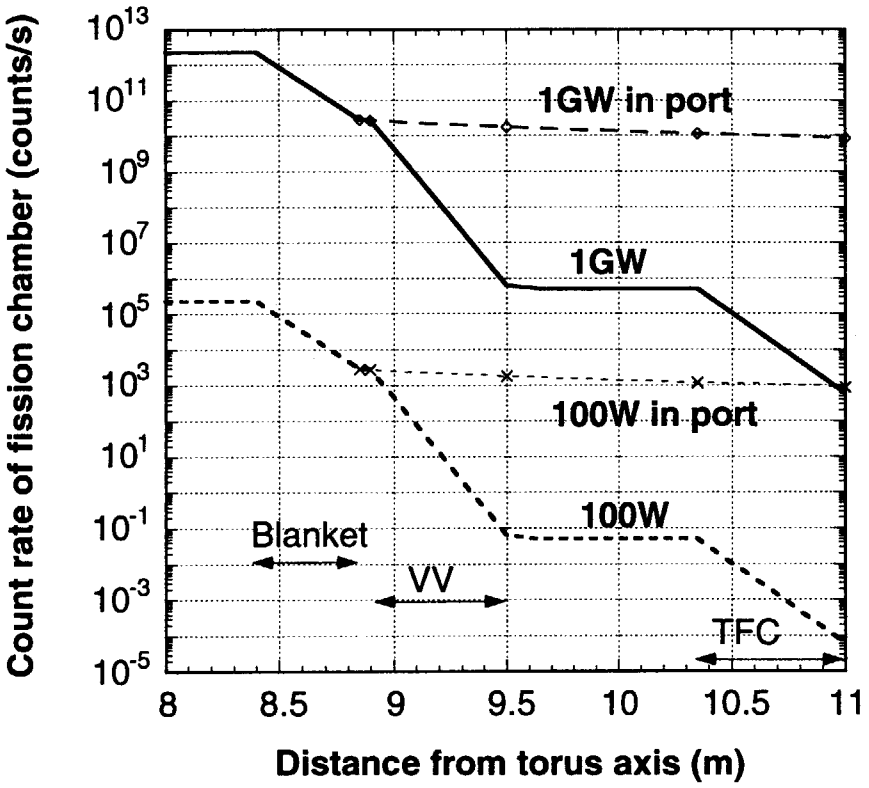

Figure 2.3-5 Count rate of the fission chamber without moderator as a function of the major radius.

2.4 Design of Moderator

The fission cross section of ^{235}U has large values for low energy neutrons and decreases with a 1/v dependence, where v is the neutron velocity. Moderated ^{235}U fission chambers feature flat energy responses across a large range of energies from 10 eV to 14 MeV. This is important to reduce the sensitivity of the detector efficiency to changes in the neutron energy spectrum. The moderator has to slow-down incident fast neutrons which have large fission cross sections. However, borated polyethylene was proposed as a moderator in the ITER-FDR design. Slowed-down neutrons will be absorbed by boron before the fission of ^{235}U. So a flat energy response could not obtained by the borated polyethylene moderator.

Figures 2.4-1, 2.4-2 and 2.4-3 show the calculated detector responses with polyethylene, graphite and beryllium moderators with 20 cm thickness, respectively. With the polyethylene moderator, the detector response decreases for low energy neutrons due to self-absorption by hydrogen. The response decreases with neutron energy for the graphite moderator, which means that the slow-down ability of graphite is not enough due to a higher mass number than hydrogen. A beryllium moderator enhances the response by (n,2n) reactions for high energy neutrons.

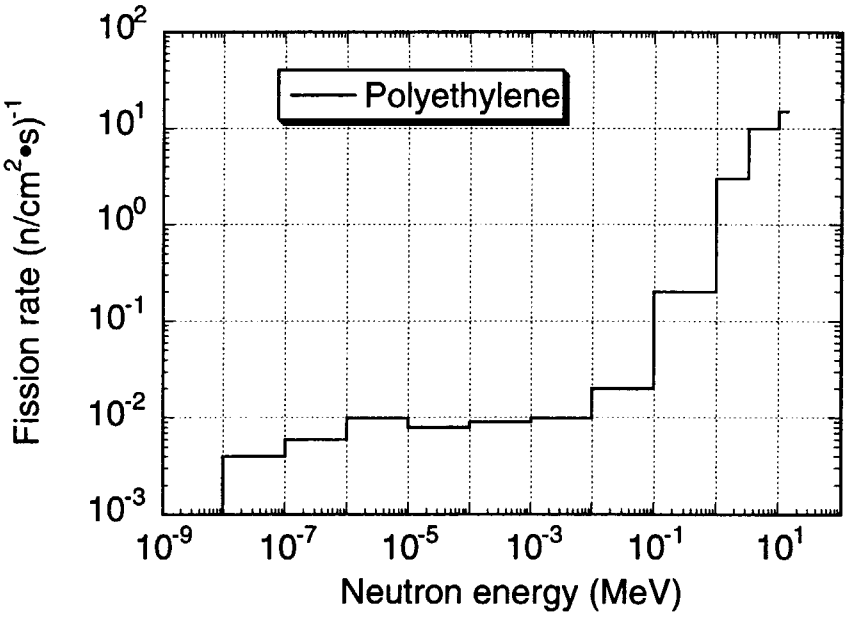

Figure 2.4-1 Calculated detector response with polyethylene moderator.

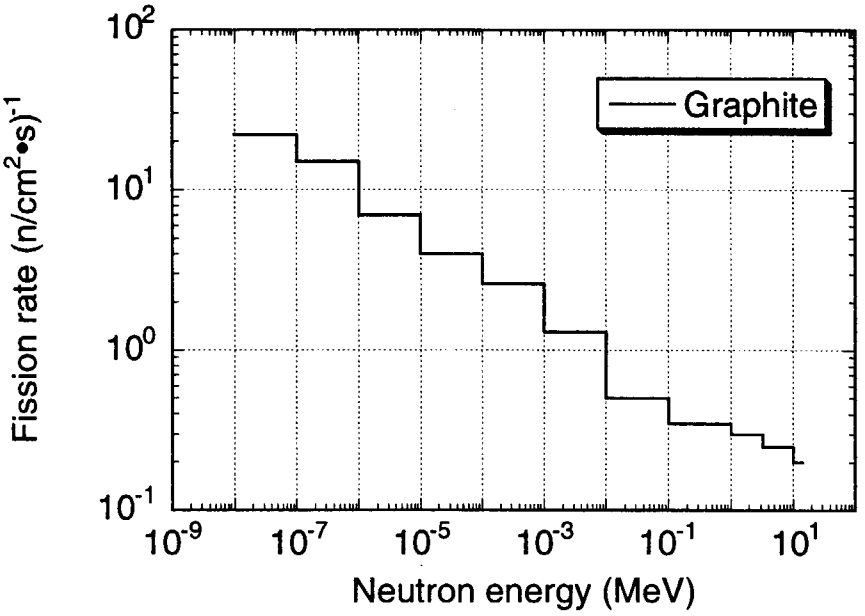

Figure 2.4-2 Calculated detector response with graphite moderator.

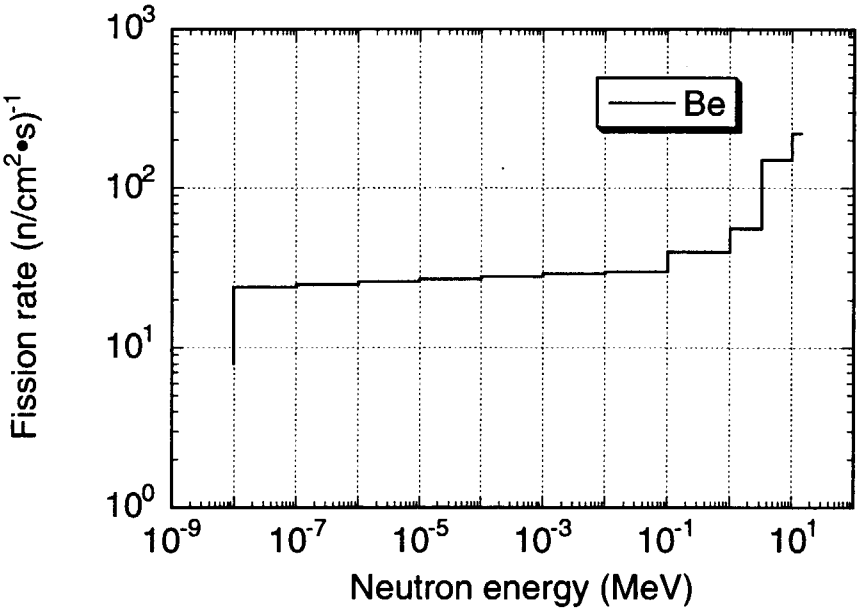

Figure 2.4-3 Calculated detector response with beryllium moderator.

In the horizontal port, the temperature will be higher than 150°C, which is the coolant water temperature. Polyethylene is not stable at such a high temperature. The temperature of the detector will be increased by nuclear heating, because the thermal conductivity of polyethylene is too small.

Here we tried to make a flat energy response by combination of graphite and beryllium. A moderator of graphite and beryllium with a ratio of Be/C=0.25 can provide rather flat energy response as shown in Fig. 2.4-4. The thermal conductivity of graphite and beryllium is much larger than that of polyethylene. Therefore we employed the moderator with graphite and beryllium with a ratio of Be/C=0.25.

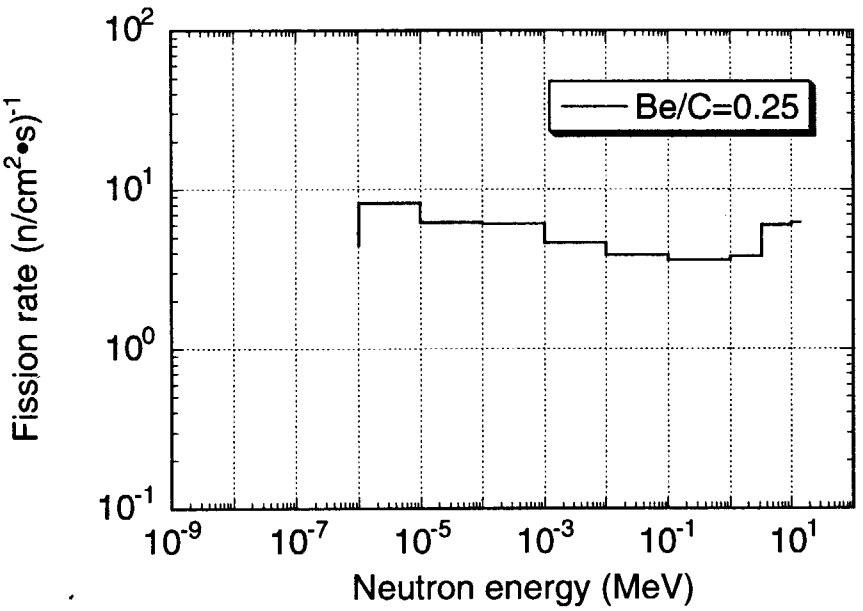

Figure 2.4-4 Calculated detector response with beryllium and carbon moderator.

2.5 Lifetime Estimation

The lifetime of the fission chamber is determined by the change of the sensitivity of the chamber due to the burn-up of the fissile material. ^{235}U is burned up through mainly fission and neutron capture reactions. The number of ^{235}U atoms N_{235U} is represented by the following equation;

$$\frac{d}{dt}N235U(t) = -N235U(t)\phi(\sigma_{f235U} + \sigma_{C235U}) \tag{2.5-1}$$

where σ_{f235U} and σ_{C235U} are averaged fission and neutron capture cross-sections defined by

$$\sigma = \frac{\int \sigma(E)\phi(E)dE}{\int \phi(E)dE} \tag{2.5-2}$$

where $\phi(E)$ is the neutron energy spectrum at the fission chamber.
From equation (2.5-1),

$$\begin{aligned} N_{235U}(t) &= N_{235U}(0)Exp\{-\phi(\sigma_{f235U} + \sigma_{C235U})t\} \\ &\approx N_{235uU}(0)\{1-\phi(\sigma_{f235U} + \sigma_{C235U})t\} \\ &\approx N_{235uU}(0)(1-t\phi\sigma_{f235U}) \end{aligned} \tag{2.5-3}$$

is obtained. Because the fission cross section is about 10^2 larger than the capture cross section for the location of the D-D detectors., the burn-up of ^{235}U atoms is dominated by fission reactions. The burn-up rate of $\phi\sigma_{f235U}$ is $\sim 2 \times 10^{-11}$ s^{-1} for the 500 MW operation. The change of the sensitivity is estimated to be only 0.1 % for the ITER lifetime which is equivalent to 0.5 GW•year. So we can use ^{235}U chambers without replacement during the ITER lifetime.

2.6 Dynamic Range

The wide dynamic range of 10^7 in a single fission chamber has been demonstrated by the JT-60U neutron monitor[3] with both pulse counting and Campbelling mode, which meets the ITER requirements for the neutron monitor. The Campbelling mode is available in the range of equivalent counting rates from 10^5 to 10^9 counts/s. Direct current mode measurement is available in the range of equivalent counting rates higher than 10^8 counts/s. Here we plan to use fission chambers in pulse counting and Campbelling modes, because the S/N ratios for the gamma induced noises in those modes are better than that of the current mode. Figure 2.6-1 shows the expected count rate of the fission chambers with moderator as a function of the fusion power. At the fusion power of 100 W, the counting rate of 4000 cps is expected in the detectors for D-D and the calibration with a moderator. The count rate of the detectors for the D-T operation is too high for the Campbelling mode at 500 MW fusion power. Therefore we have to reduce the count rate by a neutron shield.

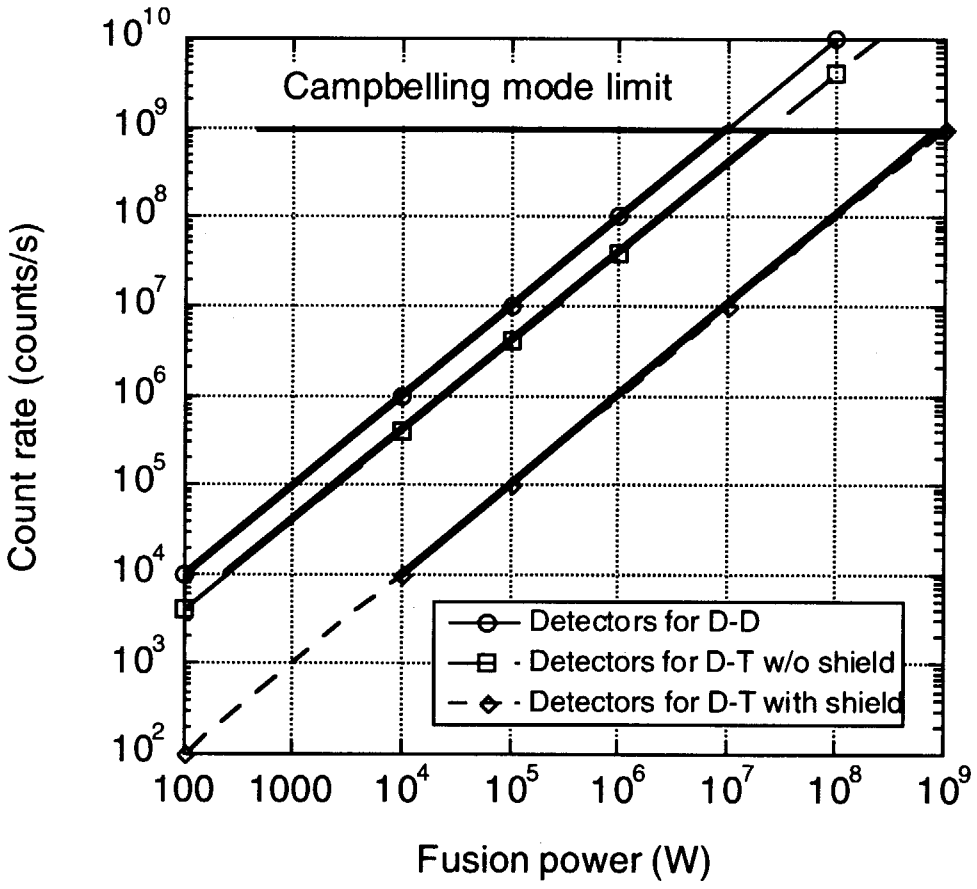

Figure 2.6-1 Dynamic range of the fission chamber with 200 mg of ^{235}U.

However, the statistical error of the pulse counting is a problem for lower fusion power. The statistical error of the pulse counting is plotted against the fusion power for 1 ms and 10 ms sampling times in Fig.2.6-2. The ITER requirement of the error in the fusion power measurement is 20% and 10% for fusion power of 100-10kW and 10k-1GW, respectively. The systematic error in the calibration for the total neutron source strength is estimated to be about 5% from the experience of the calibration for the TFTR D-T experiments. So the statistical should be less than 19.4 % and 8.7% for fusion power of 100-10kW and 10k-1GW, respectively. By combination of the detectors for the D-D and D-T operations, we can measure the total neutron flux within the errors required by ITER in the range of the fusion power from 100W to 1GW.

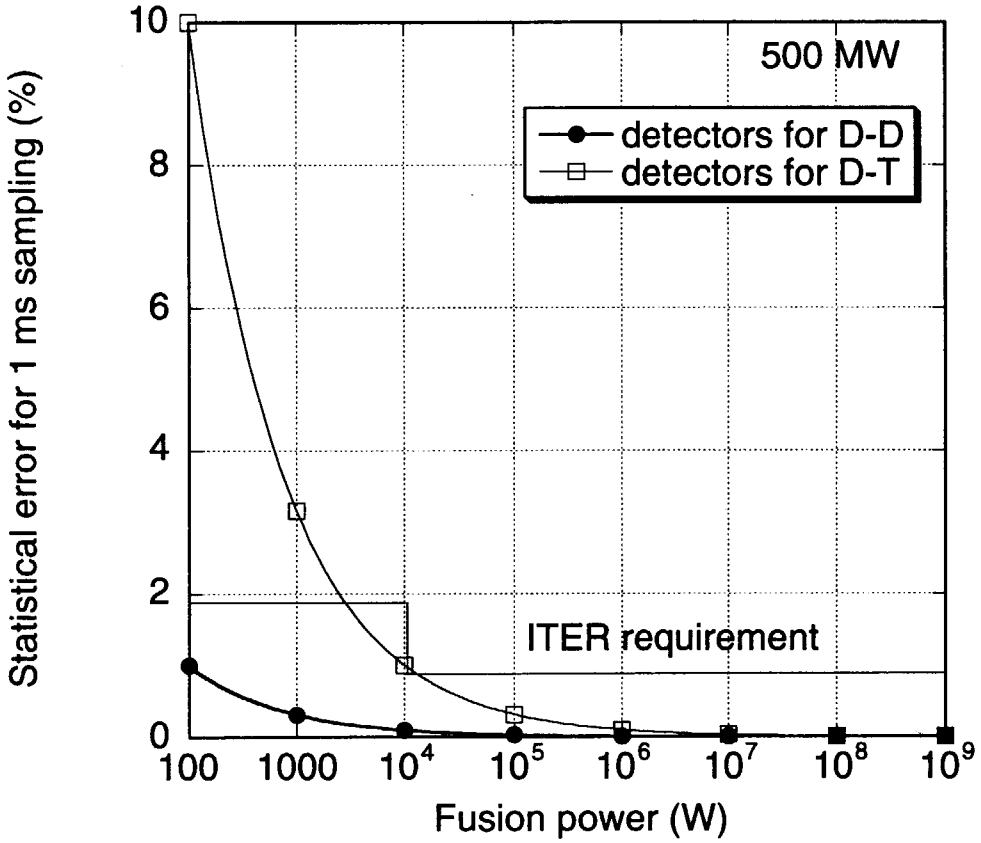

Figure 2.6-2 Statistical error of the pulse counting plotted against the fusion power for 1 ms and 10 ms sampling times.

2.7 Gamma-ray Effect

This fission chamber can be operated in the pulse counting and the Campbelling mode. In the pulse counting mode, the current pulse generated by the fission fragments or gamma reaction in the ionizing gas is measured. The fission reaction releases ~100 MeV as the kinetic energy of the fission fragments. One fragment goes into the ionization gas and another goes into the electrode wall. The average energy deposited in the ionization gas is about 43 MeV, on the other hand the gamma energy is less than 10 MeV (see Fig.2.3-3). So we can eliminate the gamma pulses by conventional pulse discrimination techniques. The Campbell mode is less sensitive to gamma-rays and the gamma-ray effect is negligible. Based on the data sheet of the fission chamber, the gamma-ray effects are summarized in Table 2.7-1. We can obtain sufficient S/N ratios for gamma-ray induced noise. Therefore we do not need a gamma-ray compensation detector which is of the same size as the detector but without fissile material..

Table 2.7-1 Outputs of the fission chamber by neutrons and gamma-rays at 500 MW operation.

	Detectors for D-D	Detectors for D-T
Neutron Flux	2×10^{16} n/m^2	3×10^{15} n/m^2
Gamma dose rate	2×10^{6} R/h	3×10^{5} R/h
Campbelling mode (A^2/Hz)		
Neutrons	1.1×10^{-14}	3.3×10^{-15}
Gammas	1.4×10^{-21}	4.2×10^{-22}
S/N ratio	1.3×10^{7}	1.3×10^{7}
Current mode (A)		
Neutrons	4.0×10^{-2}	1.2×10^{-3}
Gamma-rays	4.0×10^{-5}	1.2×10^{-6}
S/N ratio	1.0×10^{3}	1.0×10^{3}

2.8 Magnetic Field Effect

The fission chambers for the D-D operation and the calibration will be installed inside the toroidal field magnet. The effect of the strong magnetic field on the fission chamber is another problem. In the fission chamber, we measure the electron induced current from ionization by fission fragments. So we calculated the electron drift orbit in the magnetic field. The electron drift velocity u is represented by

$$\mathbf{u} = \frac{\mu_e}{1+\omega_c^2/\nu^2}\left[\mathrm{E} + \frac{\mathbf{E}\times\mathbf{B}}{\mathrm{B}}\frac{\omega_c}{\nu} + \frac{(\mathbf{E}\bullet\mathbf{B})}{\mathrm{B}^2}\frac{\omega_c^2}{\nu^2}\right] \tag{2.8-1}$$

where me is the electron mobility, n is the collision frequency of the electron to neutral atoms, and wc is the electron cyclotron frequency in the magnetic field B. If we assume E = (Ex, 0, 0) and B = (0, 0, Bz),

$$\mathbf{u} = \left(\frac{\mu_e E_x}{1+\omega_c^2/\nu^2}, \frac{\mu_e E_x}{1+\omega_c^2/\nu^2}\frac{\omega_c}{\nu}, 0\right) \tag{2.8-2}$$

As shown in Fig. 2.8-1, an angle between u and E, the Lorentz angle α, is represented by $\tan\alpha = \omega c/\nu$. In the case of the fission chamber with 8 atm Argon gas, applied voltage of 200 V to 0.5 mm electrode gap, in a magnetic field of 5.3 T, the mobility without magnetic field is $u_0 \approx 3 \times 10^3$ m/s. The Lorentz angle is evaluated as,

$$\begin{aligned}\tan\alpha &= \omega_c/\nu \\ &\approx \mathbf{u}_0(\mathrm{E}/\mathrm{E})\end{aligned} \tag{2.8-3}$$

Thus the magnetic effect on the electron drift velocity is negligible. However, we do not have

experience of using a fission chamber using in high magnetic fields such as 5.7T. We should confirm the magnetic effects on the fission chamber experimentally.

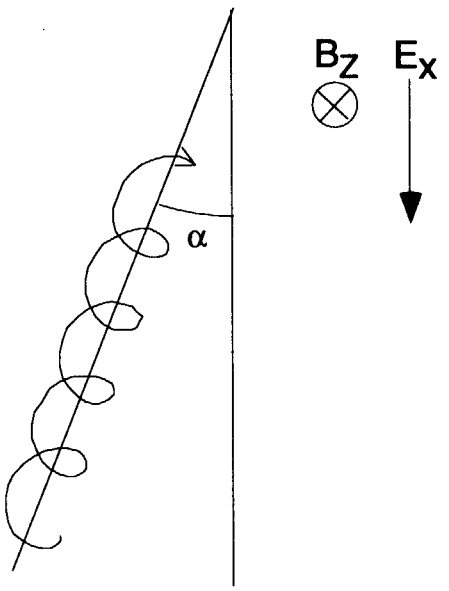

Figure 2.8-1 Lorentz angle of electron drift in a magnetic field.

2.9 Nuclear Heating

Nuclear heating of the detector is an important issue for the diagnostics inside or near the vacuum vessel. Preliminary estimation of the nuclear heating around the vacuum vessel is shown in Fig. 2.9-1. The nuclear heating of the fission chamber is estimated to be 0.1 - 0.2 W/cm^3 at the detector position. The fission chamber can be operated up to 400 °C, so that it seems possible to cool it by thermal conductivity via modulator.

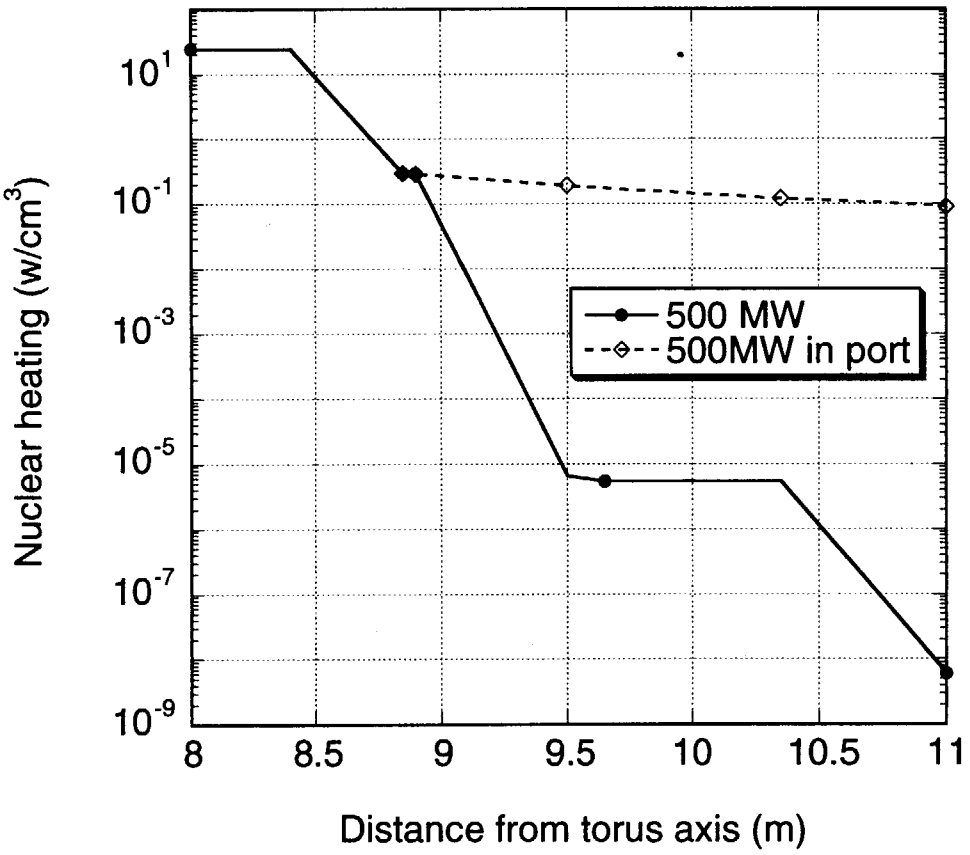

Figure 2.9-1 Preliminary estimation of the nuclear heating around the vacuum .

2.10 Calibration

Absolute calibration of the source strength monitors is the most critical issue in the design of the neutron monitor. In the present tokamaks, neutron monitors are calibrated by using a neutron source such as ^{252}Cf or a DT neutron generator in the vacuum vessel. In ITER, *in-situ* calibration by moving a DT neutron generator remotely inside the vacuum vessel should be performed.

We simulated the *in-situ* calibration by MCNP calculations, where a point source of 14 MeV neutrons is moving on the plasma axis with R = 6.2 m and Z=0.53 m as shown in Fig. 2.10-1. The ITER machine within the vacuum vessel was modeled for the calculations. The detector for the calibration is located in the horizontal port.

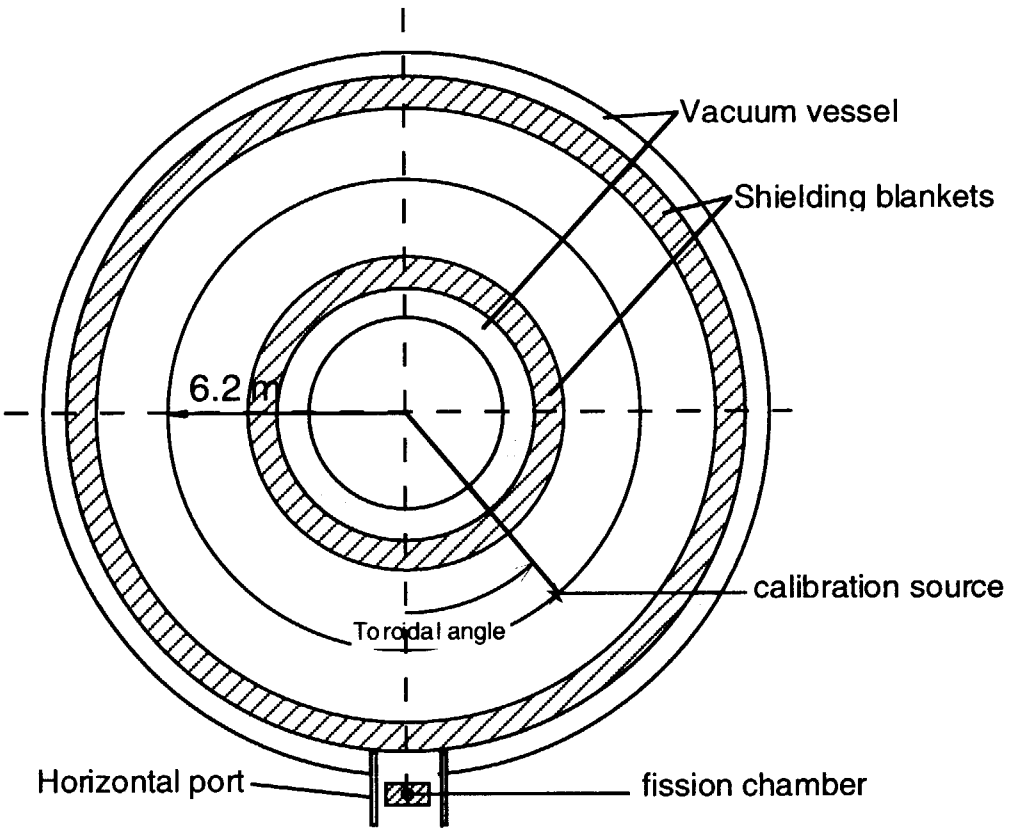

Figure 2.10-1 Calculation model of the *in-situ* calibration. A point source of 14 MeV neutrons is moving on the plasma axis with R = 6.2 m and Z=0.53 m.

Figure 2.10-2 shows the detection efficiency of the detector in the horizontal port for the point source on the plasma axis with R = 6.2 m plotted against the toroidal angle of the source. A sharp drop of the efficiency is observed at ±110°, which shows that the source goes into the shadow of the inboard blanket.

A compact DT neutron generator with an emission rate of ~10^{11} neutrons/s has been developed by the Russian home team, which can be installed on the remote handling apparatus and can move inside the vacuum vessel. If we will use the DT neutron generator with an emission rate of 1×10^{11} neutrons/s, a count rate higher than 10 count/s can be expected in the range of toroidal angles ±100 degree. Also a count rate of about 1 count/s can be expected for ±(100 - 160) degree.

The relative integrated efficiency defined by,

$$\frac{\int_0^{\phi} \varepsilon(\phi) d\phi}{\int_0^{\pi} \varepsilon(\phi) d\phi} \qquad (2.10\text{-}1)$$

where $\varepsilon(\phi)$ is a detection efficiency for a point neutron source on the plasma axis with R = 6.2 m at the toroidal angle of ϕ. The relative integrated efficiency is plotted against the toroidal angle as shown in Fig.2.10-3. In this calibration, the detection efficiency for the toroidal neutron source in derived from the integration of the detection efficiencies for a point neutron source. If we scan the point source in the range of toridal angles ±80°, we can obtain the detection efficiency for the toroidal neutron source with an accuracy higher than 95%.

An example of the calibration procedure is shown in Table 2.10-1. In this MCNP calculation, the modeling is symmetric respect to the fission chamber, however, the real ITER-FEAT machine is not symmetric. Therefore, we have to scan both toroidal directions. If we scan the point source each 10 degrees in the range of toridal angles ±180°, we need 1or 2 days for the calibration, where the time for moving the source should be taken into account.

In this design, the fission chambers are operated mainly in Campbelling mode with wide dynamic range. Here the linearity calibration of the Campbelling output is necessary before the installation. As carried out in JT-60U, the linearity calibration using a fission reactor is proposed for those fission chambers.

By those calibrations, the neutron flux monitor can meet the required 10% accuracy goals of the fusion power measurement for the ITER fusion power monitor.

Table 2.10-1 Procedure of the point source calibration.

Toroidal angle (degree)	Detection efficiency	Accumulation time (sec)	Counts	Statistical error	Relative error (%)
-180	2.882E-12	4000	1.153E+03	34.0	2.9
-170	5.231E-12	4000	2.092E+03	45.7	2.2
-160	8.852E-12	4000	3.541E+03	59.5	1.7
-150	8.508E-12	4000	3.403E+03	58.3	1.7
-140	5.247E-12	4000	2.099E+03	45.8	2.2
-130	5.398E-12	4000	2.159E+03	46.5	2.2
-120	1.367E-11	4000	5.468E+03	73.9	1.4
-110	6.301E-11	2000	1.260E+04	112.3	0.9
-100	8.745E-11	2000	1.749E+04	132.3	0.8
-90	1.001E-10	1000	1.001E+04	100.0	1.0
-80	1.210E-10	1000	1.210E+04	110.0	0.9
-70	1.037E-10	1000	1.037E+04	101.8	1.0
-60	1.187E-10	1000	1.187E+04	109.0	0.9
-50	1.533E-10	1000	1.533E+04	123.8	0.8
-40	2.400E-10	1000	2.400E+04	154.9	0.6
-30	3.478E-10	1000	3.478E+04	186.5	0.5
-20	7.485E-10	1000	7.485E+04	273.6	0.4
-10	1.692E-09	1000	1.692E+05	411.3	0.2
0	2.519E-09	1000	2.519E+05	501.9	0.2
10	1.692E-09	1000	1.692E+05	411.3	0.2
20	7.485E-10	1000	7.485E+04	273.6	0.4
30	3.478E-10	1000	3.478E+04	186.5	0.5
40	2.400E-10	1000	2.400E+04	154.9	0.6
50	1.533E-10	1000	1.533E+04	123.8	0.8
60	1.187E-10	1000	1.187E+04	109.0	0.9
70	1.037E-10	1000	1.037E+04	101.8	1.0
80	1.210E-10	1000	1.210E+04	110.0	0.9
90	1.001E-10	1000	1.001E+04	100.0	1.0
100	8.745E-11	2000	1.749E+04	132.3	0.8
110	6.301E-11	2000	1.260E+04	112.3	0.9
120	1.367E-11	4000	5.468E+03	73.9	1.4
130	5.398E-12	4000	2.159E+03	46.5	2.2
140	5.247E-12	4000	2.099E+03	45.8	2.2
150	8.508E-12	4000	3.403E+03	58.3	1.7
160	8.852E-12	4000	3.541E+03	59.5	1.7
170	5.231E-12	4000	2.092E+03	45.7	2.2
180	2.882E-12	4000	1.153E+03	34.0	2.9
	Total(hour)	23.1		Total error(%)	0.5

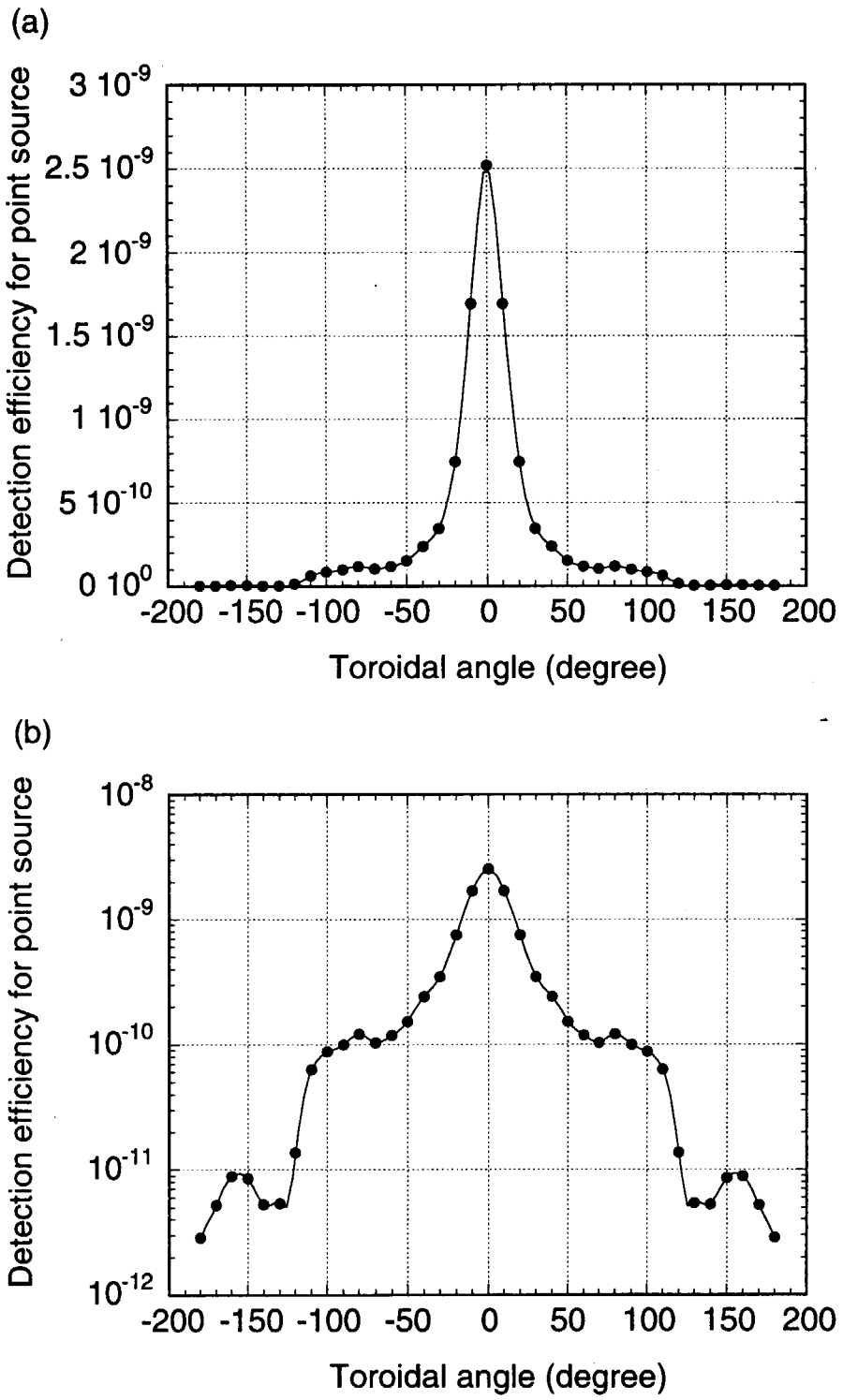

Figure 2.10-2 Detection efficiency of the detector for the D-D and the calibration against the point source on the plasma axis with R = 6.2 m plotted versus the toroidal angle of the source. (a) is a linear plot and (b) is a log plot.

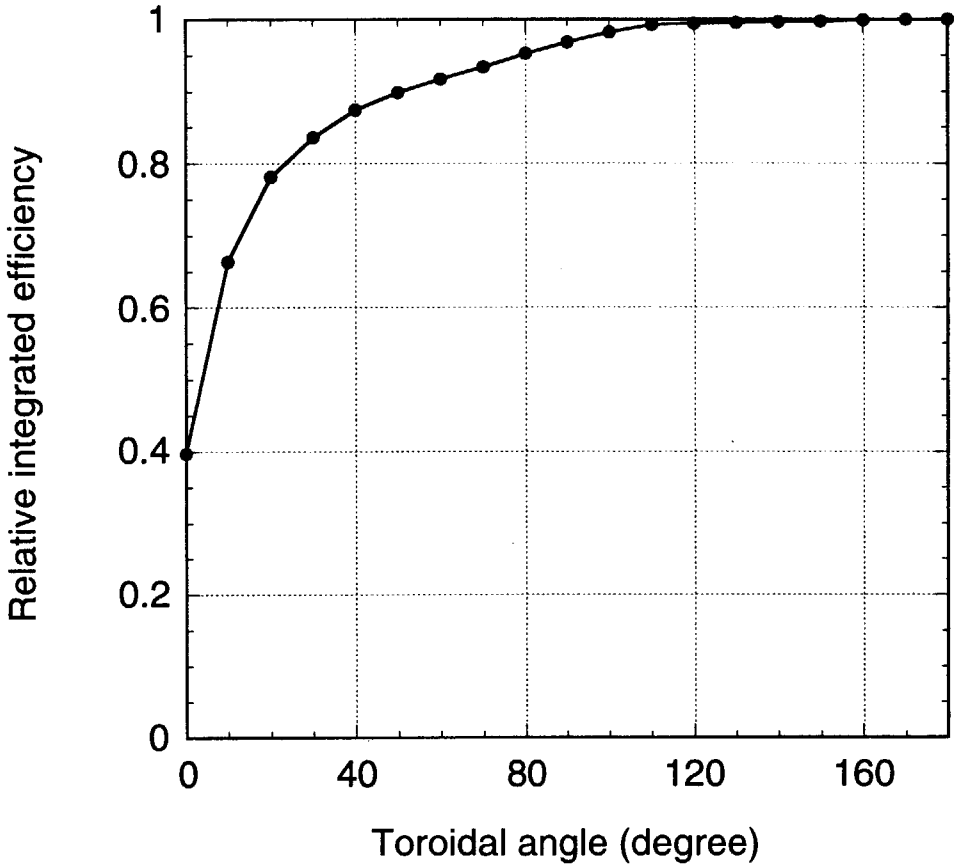

Figure 2.10-3 Relative integrated efficiency plotted against the toroidal angle.

3. DETAILED SYSTEM DESCRIPTION

3.1 General Equipment Arrangement

The proposed arrangement of neutron flux monitors on ITER-FEAT is shown in Fig. 3.1-1. The neutron flux monitors will be installed in the equatorial ports at ports #8 and #17. A pair of the fission chamber assemblies will be installed in each port; one is for D-D and calibration operation, and another is for D-T operation.

The pre-amplifier should be located as near as possible to the fission chambers from the noise protection point of view. Therefore, pre-amplifiers will be installed just outside of the cryostat. Integrated amplifiers and power supplies will be installed in the pit.

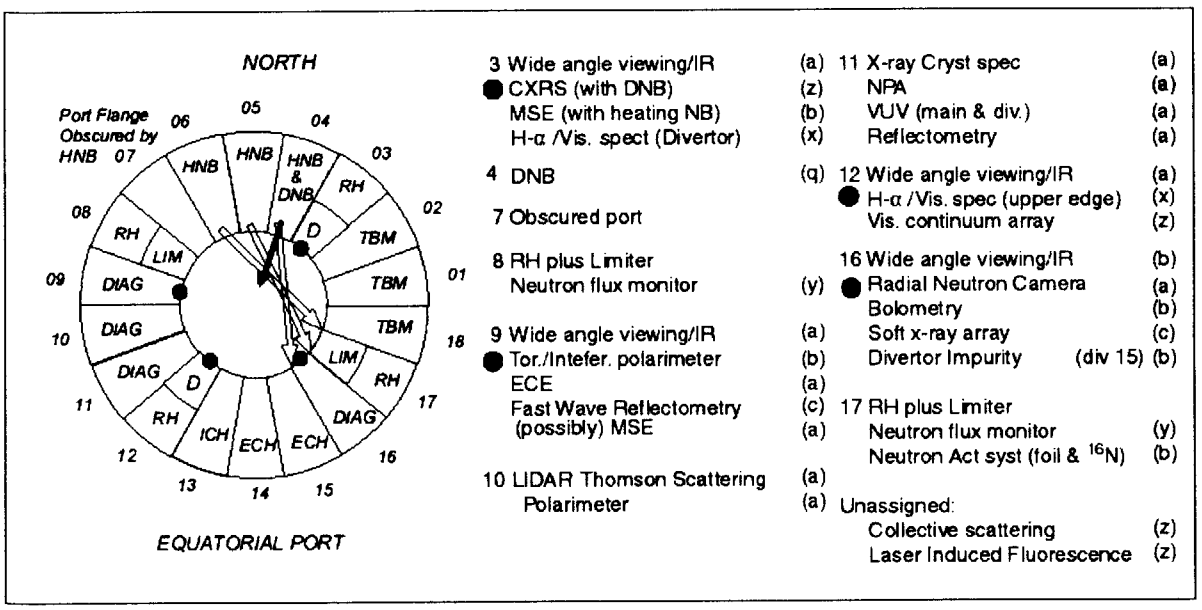

Figure 3.1.1 Diagnostics arrangement on equatorial ports. The neutron flux monitor will be installed in the equatorial ports at ports #8 and #17.

3.2 Fission Chamber Assembly

Fission chamber assembly was designed based on the calculation described in Section 2.4. Three detectors are mounted in a stainless steel housing with moderation material as shown in Fig. 3.2-1. We employed graphite for the moderator instead of polyethylene, because graphite is stable at high temperatures. We need 20-cm thick graphite and 5-cm thick beryllium to get flat energy response of the detector sensitivity. Cadmium of 1-mm thickness is plated inside the stainless steel housing for a thermal neutron shield. Three ^{235}U fission chambers with the same size are mounted inside the gamma-ray shield of lead from the redundancy point of view.

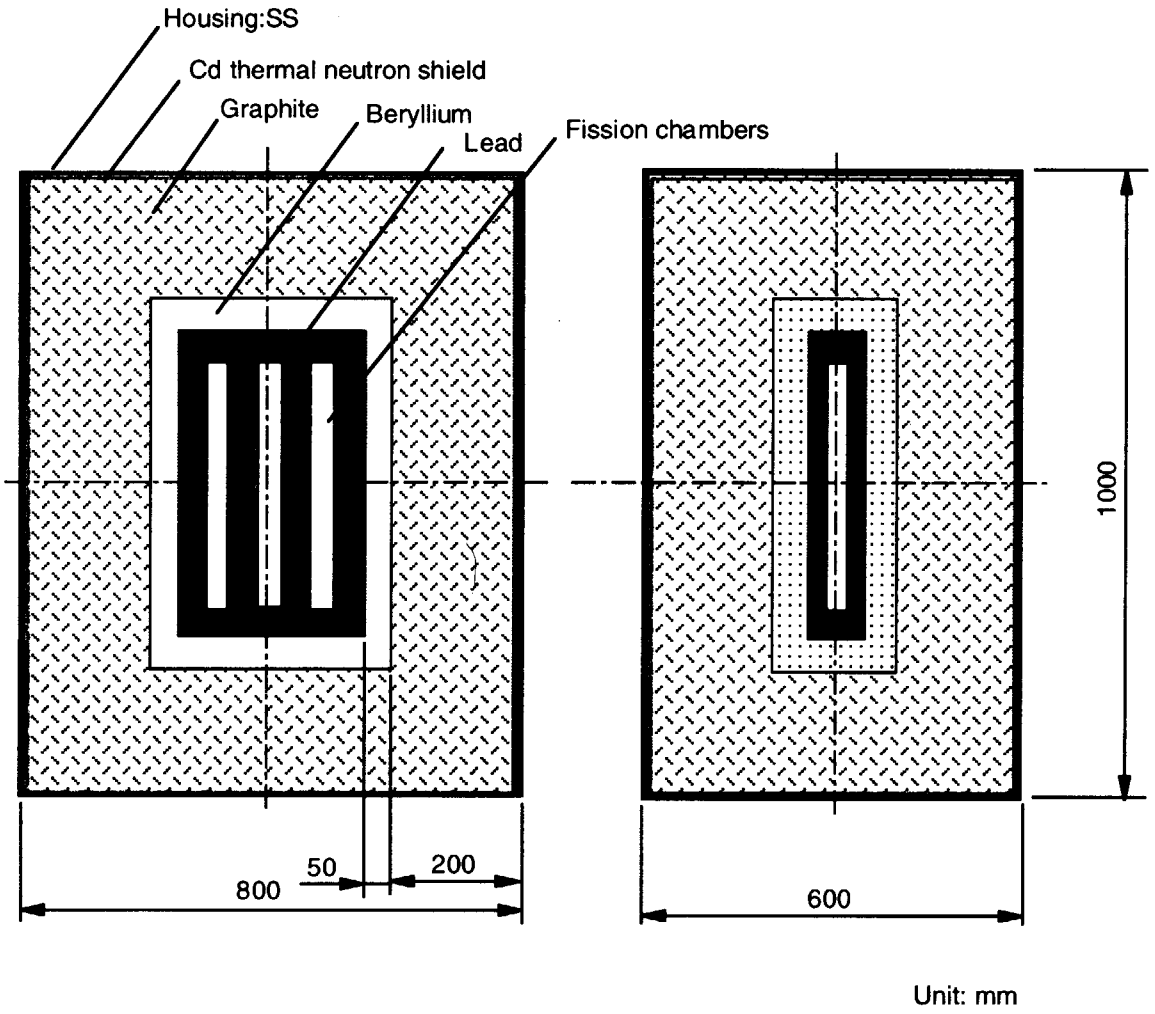

Figure 3.2-1 Schematic diagram of the fission chamber assembly with moderator.

3.3 Installation of the Fission chamber Assembly on the Equatorial Port

The arrangement of the neutron flux monitor is shown in Fig. 3.3-1. The detectors for the D-D operation and the calibration are installed just outside of the vacuum vessel in the horizontal port. The detectors for the D-T operation are installed just outside of the additional shield in the port. The additional shield in not designed yet, which should be done taking account of other diagnostics integration.

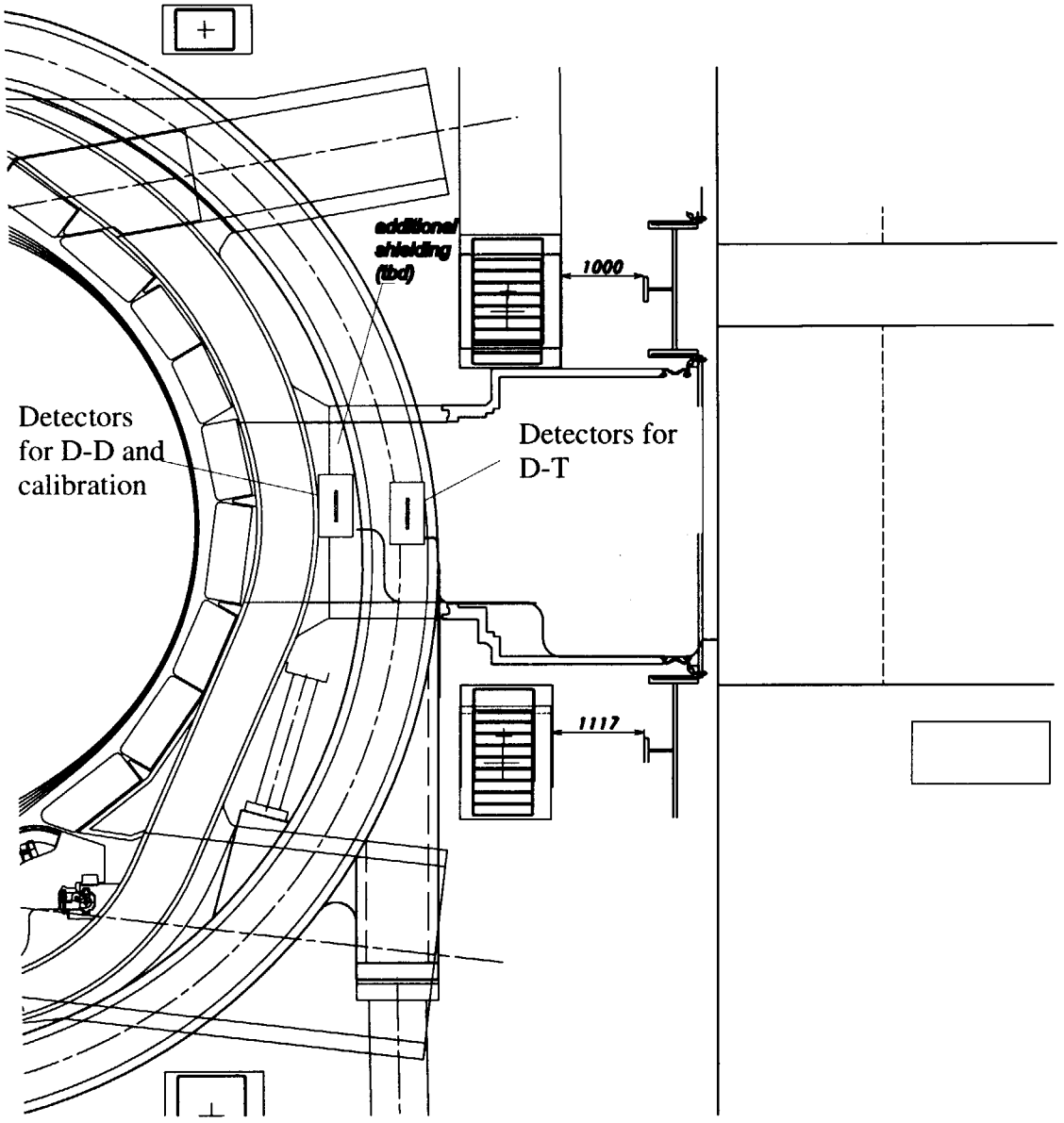

Figure 3.3-1 Arrangement of neutron flux monitors.

3.4 Data Acquisition and Control

A block diagram of the electronics and data acquisition equipment is shown in Fig.3.4-1. The detectors will require high voltage power supplies, preamplifiers, amplifiers, pulse counting circuitry, Campbelling amplifiers, digital equipment, etc. Preamplifiers should be installed near the detectors. Considering the radiation condition, a location in the pit near the biological shield is desirable. The integrated amplifier designed for the JT-60U neutron flux monitor which includes a high voltage power supply, a pulse amplifier, and a Campbelling amplifier is preferable. The Campbelling amplifier has three different amplitude outputs. Typically, the relative gains are 1, 10^2 and 10^4 to get a wide dynamic range.

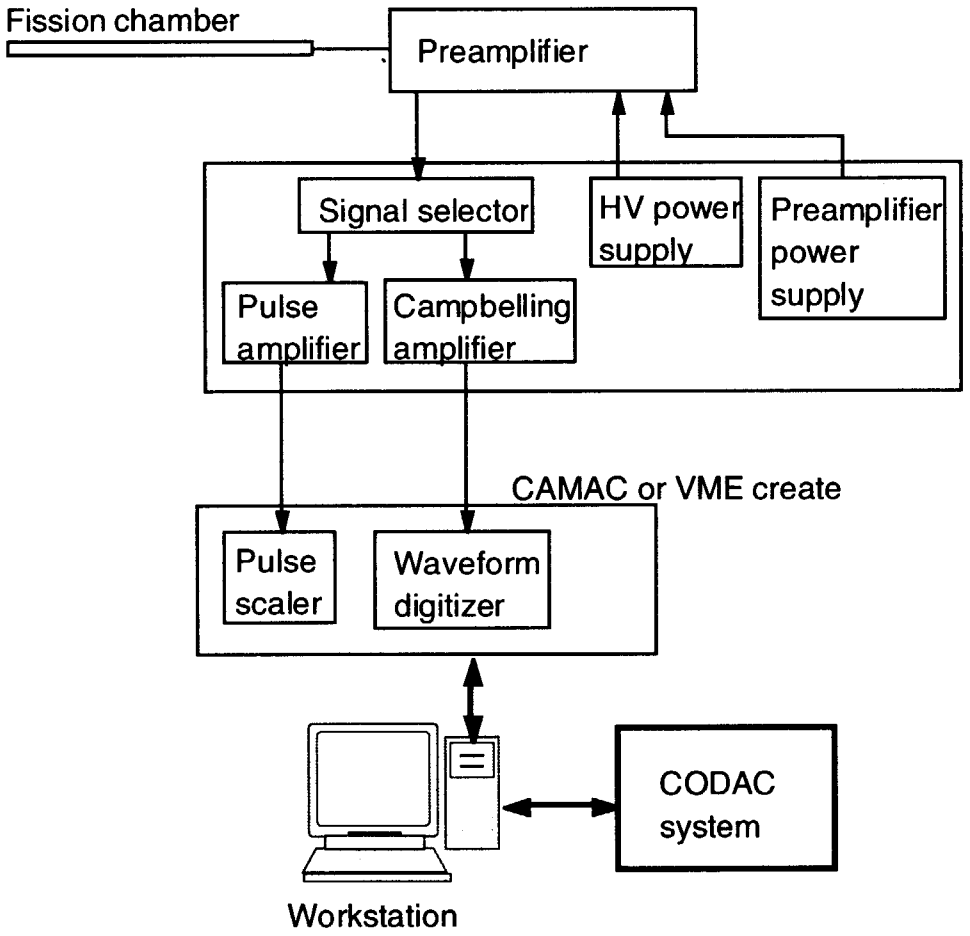

Figure 3.4-1 Block diagram of the electronics and data acquisition equipment.

The policy of the data acquisition for all diagnostics has not been established. We estimated the data amount of the fission chamber system assuming that we will measure with constant sampling time for a whole discharge as shown in Table 3.4-1.

Table 3.4-1 Data amount of the neutron flux monitor.

	# channel	Sampling time ms	Operation mode		
			Inductive	Hybrid	Non-inductive
Discharge length (sec)			400	1000	3000
			Data amount (MB)		
Pulse counting mode	12	1	9.6	24	72
Campbelling mode	36	1	57.6	144	432
Total			67.2	168	504

3.5 Calibration Hardware

As discussed in Section 2.9, *in-situ* calibration will be required to get the detection efficiencies for the total neutron source strength or the fusion power. An essential element of such calibrations is an intense, robust, yet compact DT neutron generator. The generator should produce 14 MeV neutrons at an average rate of ~10^{11} n/s, and be sufficiently compact and portable to allow operation inside the ITER vacuum vessel during initial system calibration and extended maintenance periods, using standard remote handling equipment, for *in situ* mapping of the detector response. This calibration hardware can be shared with the neutron flux monitor installed outside the vacuum vessel. So far, a neutron generator which has been developed by the Russian home team is one of the candidates [12] (see Fig.3,5-1).

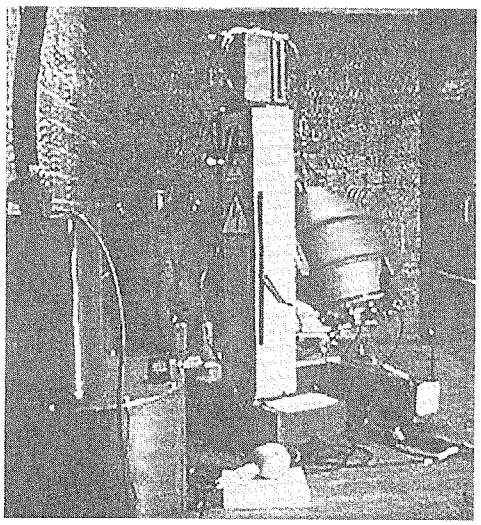

Figure 3.5-1 Picture of the neutron generator developed by TRINITI.

3.6 Component List

List of Components is summarized in Table 3.6-1.

Table 3.6-1 List of equipment

Component	Quantity	Size (mm)	weight (kg)
^{235}U Fission Chamber	12	$\phi 28 \times 390$	2.0
Detector box with moderator	4	800× 1000× 600	500
Soft Tri-axial Cable	12	$\phi 12$	
Preamplifier	12	300× 190 × 120	4
Preamplifier Box	2	600× 800 × 200	120
Integrated Amplifier	12	480× 180 × 400	10
CAMAC or VME create	2	300× 190× 120	20
ADC Module	3		
Scalar Module	1		
Workstation	1		
Other Digital Modules	TBD		
Neutron generator	1		

4. OPERATION STATE DESCRIPTION

4.1 Commissioning State

All equipment should be installed in the commissioning stage of ITER. ITER has not commenced operation. All electronic equipment is accessible for testing.

4.2 Calibration State

Neutron flux monitors are installed and operational. ITER has not commenced operation, and the vacuum vessel is open for in-vessel activities. The neutron generator and transport apparatus are temporarily installed inside the ITER vacuum vessel before initial pump-down. Personnel access is excluded in all areas affected by operation of the neutron generator.

4.3 Experimental Operations State

All equipment is operational. ITER will be in operation. Personnel access is excluded, according to project safety requirements.

4.4 Maintenance State

ITER is not in operation. Access to equipment for maintenance activities is determined according to project safety requirements. Basically equipment inside the biological shield are maintenance free.

5. CRITICAL DESIGN AREAS AND R&D ITEMS

5.1 Critical Design Areas

- Integration of the detector assembly in the equatorial port should be done.

- Analysis of the electro-magnetic stress in disruption should be done.

- Technique for the sensitivity calibration should be designed. One of the candidates is that small amount of radioactive neutron source such as ^{252}Cf will be transferred to near the fission chamber. Another candidate is a cross calibration to the neutron activation measurement which is an absolute neutron flux measurement.

- Heat transport calculations for the nuclear heating of the fission chamber should be carried out.

5.2 Necessary R&D Items

- The energy response of a fission chamber with a moderator composed of graphite and beryllium should be evaluated experimentally.

- The effect of the temperature on the sensitivity should be evaluated experimentally.

- Vibration tests on the fission chamber should be done to simulate the mechanical shock in disruptions.

- The effect of the strong RF heating on the fission chamber should be confirmed experimentally.

6. CONCLUSION

We designed a neutron flux monitor using ^{235}U fission chambers to be installed inside the horizontal port. In the ITER-FDR design, a moderator of polyethylene was proposed, which is not stable in high temperature. We investigated other moderator materials to get flat energy responses of ^{235}U fission chambers. Here we employed a moderator composed of graphite and beryllium with a ratio of Be/C=0.25. These materials are stable at ITER relevant temperature in a horizontal port. Based on the neutronics calculation, a fission chamber with 200 mg of ^{235}U is adopted for the neutron flux monitor. Three detectors are mounted in a stainless steel housing with moderation material. The neutron flux monitors will be installed in the equatorial ports at ports #8 and #17. Two fission chamber assemblies will be installed in each port; one is for D-D and calibration operation, and another is for D-T operation. The assembly for the D-D operation and the calibration is installed just outside of the vacuum vessel in the horizontal port. The assembly for the D-T operation is installed just outside the additional shield in the port. Combining these assemblies with both pulse counting mode and Campbelling mode in the electronics, we can accomplish the ITER requirement dynamic range of 10^7 with 1 ms temporal resolution. The lifetime of the fission chamber was estimated. The change of the sensitivity due to burn-up of ^{235}U was estimated to be only 0.1 % behind the port plug for the ITER lifetime. So we can use ^{235}U chambers without replacement during the ITER lifetime. The effects of gamma-rays and magnetic fields on the fission chamber are negligible in this arrangement. We simulated the *in-situ* calibration by MCNP calculations, where a point source of 14 MeV neutrons is moving on the plasma axis. It was found that direct calibration would be possible by using a neutron generator with an intensity of 10^{11} n/s. The neutron flux monitor can meet the required 10% accuracy for a fusion power monitor.

ACKNOWLEDGMENTS

The authors would like to appreciate Mr. H. Kawasaki and Mr. M. Wada for their support on the neutronics calculations. We appreciate Drs. Cris Barnes and L.C. Johnson for their work on the neutron flux monitor for ITER FDR.

This report has been prepared as an account of work assigned to the Japanese Home Team under Task Agreement number N 55 TD 02.03 FJ within the Agreement among the European Atomic Energy Community, the Government of Japan, and the Government of the Russian Federation on Cooperation in the Engineering Design Activities for the International Thermonuclear Experimental Reactor ("ITER EDA Agreement") under the auspices of the International Atomic Energy Agency (IAEA).

REFERENCES

[1] O.N. Jarvis, G. Sadler, P. van Bell and T. Elevant, In-vessel calibration of the JET neutron monitors using a ^{252}Cf neutron source: Difficulties experienced, Rev. Sci. Instrum. 61: 3172 (1990).

[2] H.W. Hendel, R.W. Palladino, Cris W. Barnes, et al., In situ calibration of TFTR neutron detectors, Rev. Sci. Instrum. 61: 1900 (1990).

[3] T. Nishitani, H. Takeuchi, T. Kondoh, et al., Absolute calibration of the JT-60U neutron monitors using a ^{252}Cf neutron source, Rev. Sci. Instrum. 63: 5270 (1992).

[4] V.Mukhovatov, H. Hopman, S. Yamamoto, et al., in: ITER Diagnostics, ITER Documantation Series, No.33, IAEA, Vienna (1991).

[5] T. Iguchi, J. Kaneko, M. Nakazawa, T. Matoba, T. Nishitani and S. Yamamoto, Conceptional design of neutron diagnostics system for fusion experimental reactor, Fusion Eng. Design 28: 689 (1995).

[6] T. Nishitani, K. Ebisawa, T. Iguchi and T. Matoba, Design of ITER neutron yield monitor using microfission chambers, Fusion Eng. Design 34-35: 567 (1997).

[7] T. Nishitani, K. Ebisawa, L.C. Johnson, et al., In-Vessel Neutron Monitor Using Micro Fission Chambers for ITER, in: Diagnostics for Experimental Thermonuclear Fusion Reactor 2, P.E. Stott, G. Gorini and E. Sindoni ed., Plenum Press, New York (1998).

[8] T. Nishitani, S. Kasai, L.C. Johnson, K. Ebisawa, C. Walker and T. Ando. Neutron monitor using microfission chambers for the International Thermonuclear Fusion Reactor, rev. Sci. Instrum. 70: 1141 (1999).

[9] Y. Endo, T. Ito and E. Seki, A counting-Cambelling neutron measurement system and its experimental results by test reactor, IEEE Trans. Nucl. Sci. NS-29: 714 (1982).

[10] Briesmeister J. F. (Ed.): "MCNP - A General Monte Carlo N-Particle Transport Code, version 4B," LA-12625-M, Version 4B, Los Alamos National Laboratory (1997).

[11] T. Nakagawa, K. Shibata, S. Chiba, et al., Japanese evaluated nuclear data library version 3 revision-2: JENDL-3.2, J. Nucl. Sci. Technol. 32: 1259(1995).

[12] Yu.A. Kaschuck, D.V. Portnov, A.V. Krasilnikov, et al., Compact Neutron Generator for Diagnostic Applications, Rev. Sci. Instrum. 70:1104 (1999).

This is a blank page.

国際単位系 (SI) と換算表

表 1　SI 基本単位および補助単位

量	名称	記号
長さ	メートル	m
質量	キログラム	kg
時間	秒	s
電流	アンペア	A
熱力学温度	ケルビン	K
物質量	モル	mol
光度	カンデラ	cd
平面角	ラジアン	rad
立体角	ステラジアン	sr

表 2　SI と併用される単位

名称	記号
分，時，日	min，h，d
度，分，秒	°，′，″
リットル	l，L
トン	t
電子ボルト	eV
原子質量単位	u

1 eV = 1.60218 × 10^{-19} J

1 u = 1.66054 × 10^{-27} kg

表 5　SI 接頭語

倍数	接頭語	記号
10^{18}	エクサ	E
10^{15}	ペタ	P
10^{12}	テラ	T
10^{9}	ギガ	G
10^{6}	メガ	M
10^{3}	キロ	k
10^{2}	ヘクト	h
10^{1}	デカ	da
10^{-1}	デシ	d
10^{-2}	センチ	c
10^{-3}	ミリ	m
10^{-6}	マイクロ	μ
10^{-9}	ナノ	n
10^{-12}	ピコ	p
10^{-15}	フェムト	f
10^{-18}	アト	a

表 3　固有の名称をもつ SI 組立単位

量	名称	記号	他の SI 単位による表現
周波数	ヘルツ	Hz	s^{-1}
力	ニュートン	N	m·kg/s^2
圧力，応力	パスカル	Pa	N/m^2
エネルギー，仕事，熱量	ジュール	J	N·m
工率，放射束	ワット	W	J/s
電気量，電荷	クーロン	C	A·s
電位，電圧，起電力	ボルト	V	W/A
静電容量	ファラド	F	C/V
電気抵抗	オーム	Ω	V/A
コンダクタンス	ジーメンス	S	A/V
磁束	ウェーバ	Wb	V·s
磁束密度	テスラ	T	Wb/m^2
インダクタンス	ヘンリー	H	Wb/A
セルシウス温度	セルシウス度	℃	
光束	ルーメン	lm	cd·sr
照度	ルクス	lx	lm/m^2
放射能	ベクレル	Bq	s^{-1}
吸収線量	グレイ	Gy	J/kg
線量当量	シーベルト	Sv	J/kg

表 4　SI と共に暫定的に維持される単位

名称	記号
オングストローム	Å
バーン	b
バール	bar
ガル	Gal
キュリー	Ci
レントゲン	R
ラド	rad
レム	rem

1 Å = 0.1 nm = 10^{-10} m

1 b = 100 fm^2 = 10^{-28} m^2

1 bar = 0.1 MPa = 10^5 Pa

1 Gal = 1 cm/s^2 = 10^{-2} m/s^2

1 Ci = 3.7 × 10^{10} Bq

1 R = 2.58 × 10^{-4} C/kg

1 rad = 1 cGy = 10^{-2} Gy

1 rem = 1 cSv = 10^{-2} Sv

（注）

1. 表 1 − 5 は「国際単位系」第 5 版，国際度量衡局 1985 年刊行による。ただし，1 eV および 1 u の値は CODATA の 1986 年推奨値によった。
2. 表 4 には海里，ノット，アール，ヘクタールも含まれているが日常の単位なのでここでは省略した。
3. bar は，JIS では流体の圧力を表わす場合に限り表 2 のカテゴリーに分類されている。
4. EC 閣僚理事会指令では bar，barn および「血圧の単位」mmHg を表 2 のカテゴリーに入れている。

換　算　表

力	N(=10^5 dyn)	kgf	lbf
	1	0.101972	0.224809
	9.80665	1	2.20462
	4.44822	0.453592	1

粘　度　1 Pa·s(N·s/m^2) = 10 P(ポアズ)(g/(cm·s))

動粘度　1 m^2/s = 10^4 St(ストークス)(cm^2/s)

圧力	MPa(=10 bar)	kgf/cm^2	atm	mmHg(Torr)	lbf/in^2(psi)
	1	10.1972	9.86923	7.50062 × 10^3	145.038
	0.0980665	1	0.967841	735.559	14.2233
	0.101325	1.03323	1	760	14.6959
	1.33322 × 10^{-4}	1.35951 × 10^{-3}	1.31579 × 10^{-3}	1	1.93368 × 10^{-2}
	6.89476 × 10^{-3}	7.03070 × 10^{-2}	6.80460 × 10^{-2}	51.7149	1

エネルギー・仕事・熱量	J(=10^7 erg)	kgf·m	kW·h	cal(計量法)	Btu	ft·lbf	eV
	1	0.101972	2.77778 × 10^{-7}	0.238889	9.47813 × 10^{-4}	0.737562	6.24150 × 10^{18}
	9.80665	1	2.72407 × 10^{-6}	2.34270	9.29487 × 10^{-3}	7.23301	6.12082 × 10^{19}
	3.6 × 10^6	3.67098 × 10^5	1	8.59999 × 10^5	3412.13	2.65522 × 10^6	2.24694 × 10^{25}
	4.18605	0.426858	1.16279 × 10^{-6}	1	3.96759 × 10^{-3}	3.08747	2.61272 × 10^{19}
	1055.06	107.586	2.93072 × 10^{-4}	252.042	1	778.172	6.58515 × 10^{21}
	1.35582	0.138255	3.76616 × 10^{-7}	0.323890	1.28506 × 10^{-3}	1	8.46233 × 10^{18}
	1.60218 × 10^{-19}	1.63377 × 10^{-20}	4.45050 × 10^{-26}	3.82743 × 10^{-20}	1.51857 × 10^{-22}	1.18171 × 10^{-19}	1

1 cal = 4.18605 J(計量法)

= 4.184 J　(熱化学)

= 4.1855 J　(15 °C)

= 4.1868 J(国際蒸気表)

仕事率　1 PS(仏馬力)

= 75 kgf·m/s

= 735.499 W

放射能	Bq	Ci
	1	2.70270 × 10^{-11}
	3.7 × 10^{10}	1

吸収線量	Gy	rad
	1	100
	0.01	1

照射線量	C/kg	R
	1	3876
	2.58 × 10^{-4}	1

線量当量	Sv	rem
	1	100
	0.01	1

（86 年 12 月 26 日現在）

Design of Ex-vessel Neutron Monitor for ITER